ECS Journal of Solid State Science and Technology

Point-of-Care Detection of HER2 and CA 15-3 in Breast Cancer Patients: Dual-Channel Biosensor Implementation

To cite this article: Hsiao-Hsuan Wan *et al* 2024 *ECS J. Solid State Sci. Technol.* **13** 057003

ECS Journal of Solid State Science and Technology, 2024 **13** 057003
2162-8777/2024/13(5)/057003/5/$40.00 © 2024 The Electrochemical Society ("ECS"). Published on behalf of ECS by IOP Publishing Limited

Point-of-Care Detection of HER2 and CA 15-3 in Breast Cancer Patients: Dual-Channel Biosensor Implementation

Hsiao-Hsuan Wan,[1,*] Haochen Zhu,[1] Chao-Ching Chiang,[1,*] Xinyi Xia,[1] Jian-Sian Li,[1,*] Fan Ren,[1,*,,z] Cheng-Tse Tsai,[2] Yu-Te Liao,[2] Tai-Cheng Chou,[3] Dan Neal,[4] and Josephine F. Esquivel-Upshaw[5]**

[1]*Department of Chemical Engineering, University of Florida, Gainesville, Florida 32611, United States of America*
[2]*Department of Electronics and Electrical Engineering, National Yang Ming Chiao Tung University, Hsinchu 30010, Taiwan*
[3]*TaiDoc Technology Corporation, New Taipei City 24888, Taiwan*
[4]*Department Surgery, University of Florida, Gainesville, Florida 32611, United States of America*
[5]*Department of Restorative Dental Science, Division of Prosthodontics, University of Florida, Gainesville, Florida 32611, United States of America*

Breast cancer remains a considerable health challenge, affecting numerous individuals annually. This research introduces an innovative method for detecting breast cancer utilizing dual-channel test strips capable of simultaneously assessing two key biomarkers—HER2 and CA 15-3. The test strip utilized in this study is not only cost-effective but also entirely non-invasive. The reusable device employs a printed circuit board with metal-oxide-semiconductor field-effect transistor amplification and Arduino-based control to convert voltage signals from test strips into digital readings efficiently. The device utilizes double-pulse measurement instead of direct current, effectively mitigating the screening effect. The detection limit for both biomarkers is exceptionally low at 10^{-15} g ml^{-1}, surpassing commercial enzyme-linked immunoassay kits by four orders of magnitude. The sensor demonstrates remarkable sensitivity, with 78/dec for HER2 and 56/dec for CA 15-3. Human sample tests were conducted to validate the efficacy of the dual-channel strip, successfully distinguishing between healthy and cancerous groups. The results reveal significant p-values for both HER2 and CA 15-3 tests, underscoring the significance of this research. Note that this is a rapid testing process, completed in less than 2 s. These findings offer a promising avenue for swift and accurate breast cancer detection, furnishing crucial insights for early diagnosis and subsequent treatment.
 [DOI: 10.1149/2162-8777/ad4ac4]

Manuscript submitted April 4, 2024; revised manuscript received April 25, 2024. Published May 21, 2024.

Breast cancer is the most common form of cancer among women. Each year, in the United States, roughly 240,000 women and 2,100 men confront the diagnosis of breast cancer, resulting in approximately 42,000 women and 500 men succumbing to the disease. Noteworthy is that 24% of these cases involve individuals from Black, Indigenous, or People of Color communities.[1,2] In 2023, an estimated 300,590 new cases and 43,700 deaths were recorded, reflecting an annual increase of 0.5%.[3,4] The financial toll of cancer treatments was evident in 2018, with patients shelling out a staggering $5.6 billion for interventions like surgery, chemotherapy, and radiation therapy. By 2015, the burden on the US healthcare system reached an estimated $183 billion for cancer-related care, a figure expected to soar to $246 billion by 2030.[5] When factoring in healthcare expenses and lost productivity, the annual economic impact balloons to $1.16 trillion. Notably, late cancer diagnosis amplifies the financial strain by up to sevenfold compared to early detection, underscoring the critical importance of timely diagnosis and intervention.[6]

Several detection methods have been developed, encompassing biopsy-based, biosensor-based, biomarker-based, image screening-based, and microwave breast imaging approaches.[7,8] Each of the methods mentioned above has its own advantages and disadvantages. As an illustration, mammography, while widely accessible, poses the drawback of radiation exposure and may induce discomfort in many. In women with dense breast tissue, mammography can yield unreliable results. In contrast, ultrasound is radiation-free; however, it has limitations in detecting small tumors and relies heavily on the operator's proficiency. On the other hand, Magnetic Resonance Imaging (MRI) is characterized by its heightened sensitivity, yet it comes with the trade-offs of being more costly and more time-consuming in comparison to other modalities.[9–13] The aforementioned screening methods pose challenges due to their invasive nature and high costs, presenting barriers to accessibility, particularly in resource-constrained settings such as developing countries. Therefore, there is a pressing need to innovate non-invasive and affordable approaches for breast cancer screening tests.

Human epidermal growth factor receptor-2 (HER2/erbB2) and CA 15-3 (MUC1) are two commonly used biomarkers in breast cancer detection with enzyme-linked immunoassay (ELISA).[14–16] The biomarkers can be detected not only in serum but also in saliva. Numerous studies had been done with saliva samples.[14,17–22] Belonging to a family of four transmembrane receptors, the HER2 actively participates in signal transduction pathways responsible for orchestrating cellular growth and differentiation. An upregulation or amplification of HER2 emerges as a distinctive feature associated with malignancy, signaling an unfavorable prognosis in the context of breast cancer.[23] It has been reported that CA 15-3 in saliva carries significant diagnostic value for breast cancer.[24] Identified as the first breast cancer-associated antigen in 1984, CA 15-3, a transmembrane glycoprotein, has drawn attention for its potential diagnostic role.[25] Subsequent research revealed that CA 15-3 in breast secretions not only serves as a differentiator between malignant breast cancers and benign breast diseases but also proves to be a more valuable biomarker for diagnosing breast cancer when compared with mammography.[24]

A technique with a reusable printed circuit board (PCB) containing a MOSFET and disposable single-channel test strips were employed in our previous work.[26] The method delivers results in under 2 s, making it an expedited testing process. The similar method has also been used to detect cerebrospinal fluid (CSF), cardiac troponin I, COVID-19 and Zika virus.[27–32] Sensitivity refers to the reduction in digital readings corresponding to a one-order increase in protein concentration. Logarithmic scales offer practical utility by condensing a broad spectrum of values into a more easily comprehensible scale. The sensitivity of the HER2 strip was 70/dec while the CA15-3 strip was 30/dec in the previous work. The limit of detection is down to 10^{-15} g/ml for both kinds of strips, which is four-orders lower than the commercial ELISA kits.[33,34] The contribution of this work significantly impacts the field of breast cancer detection.

Enhancing the efficacy of the detection approach involves the introduction of a novel strip design known as the double-channel

*Electrochemical Society Student Member.
**Electrochemical Society Fellow.
[z]E-mail: fren@che.ufl.edu

strip. This innovative design incorporates two distinct biomarkers, HER2 and CA 15-3, functionalized within the dual channels of the strip. This dual-biomarker approach enables simultaneous testing, thereby amplifying the precision of the rapid breast cancer test for improved accuracy.

The global breast cancer diagnostics market, valued in the billions of dollars, is continuously growing due to the increasing incidences of breast cancer worldwide.[35,36] The introduction of the double-channel strip for breast cancer detection addresses critical gaps in both market and research domains. It meets the market demand for rapid, accurate, and accessible diagnostic solutions, particularly in regions with limited healthcare infrastructure. Simultaneously, it caters to the research demand for more sensitive and specific approaches by integrating dual biomarkers, HER2 and CA 15-3, thereby enhancing detection accuracy. This innovative technology holds the promise of transforming cancer diagnostics, ultimately leading to improved patient outcomes and alleviating the burden on global healthcare systems.[37]

Experimental

The disposable dual-channel test strips are manufactured by TaiDoc Technology Corporation in Taiwan, as illustrated in Fig. 1. To create these strips, a process involving gold sputtering is initiated, followed by the selective removal of a portion of the gold to form distinct electrodes. Each channel comprises two gold electrodes, one designed for signal input and the other for signal output. Both of these electrodes within the channel are functionalized for the detection of specific biomarkers. The functionalization step is shown in Fig. 2. This functionalization enables the strips to discern variations between samples. The details of the functionalization method have been previously elucidated.[26,38–40] A solution of 10 mM thioglycolic acid (TGA) was employed to establish a robust Au-S bond, with N, N'-Dicyclohexylcarbodiimide (DCC) and N-Hydroxysuccinimide (NHS) aiding in the formation of an amide bond. This amide bond is crucial for interaction with accessible amino groups on an antibody. For the dual-channel strip, the anti-HER2/ERBB2 monoclonal antibody (Sino Biological Inc., Chesterbrook, PA) is injected into one channel, while the CA 15-3 monoclonal antibody (Sino Biological Inc., Chesterbrook, PA) is introduced into the other. Subsequently, the strips are sealed and stored in a disk at 4 °C for 18 h. Lastly, ethanolamine is employed to deactivate the un-functionalized groups, thus preventing potential interference. We conducted experiments using sensor strips that had been functionalized with HER2 antibodies to detect various CA 15-3 proteins and vice versa, employing strips functionalized with CA 15-3 antibodies to identify HER2. Notably, in both cases, there was no discernible response, and the output readings closely resembled those obtained from blank saliva samples.

Human HER2/ ErbB2/ CD340(676–1255) protein (Sino Biological Inc., Chesterbrook, PA) and human Mucin-1/ MUC-1 (CA 15-3) protein (Sino Biological Inc., Chesterbrook, PA) were diluted into a series of protein standard solution in artificial saliva (Pickering Laboratories Inc., Mountain View, CA) to obtain the calibration curve. A total of 16 human saliva samples were sourced from both breast cancer patients and healthy volunteers, facilitated by the University of Florida Clinical and Translational Science Institute (UF CTSI) Biorepository. The specimens were collected from individuals within the UF Health System and have been meticulously preserved in a deep-freeze storage unit at −78 °C. All of these samples were de-identified and accompanied by corresponding diagnoses, which were rigorously validated through biopsy procedures conducted as part of the patients' routine medical care (UF IRB202101643). After thawing the saliva samples, the samples were directly introduced into the microfluidic channel without the need for any dilution, filtration, or centrifugation steps. Categorizing the human samples based on their histologic type, we distinguished them into three distinct groups: (1) healthy control, (2) in situ breast cancer, and (3) invasive breast cancer. Among the invasive breast cancer samples, one was identified as HER2 positive, while the remaining samples were HER2 negative, as confirmed by immunohistochemistry (IHC) results from biopsy analyses. We conducted tests on all the samples using the two channels on the strip, functionalized with HER2 and CA 15-3 antibodies respectively. The p-values of the testing results were analyzed by Kruskal-Wallis tests (continuous outcomes) and Fisher's exact tests. The Kruskal-Wallis test stands as a robust non-parametric technique utilized to ascertain significant differences among two or more groups, showcasing resilience even with limited sample sizes.[41,42] Complementing this, Fisher's exact test emerges as a crucial asset in cancer data examination, adept at analyzing contingency tables, especially when dealing with small sample sizes and categorical variables.[43] Its application spans across numerous medical studies, evaluating the relationship between various factors and cancer outcomes.[44]

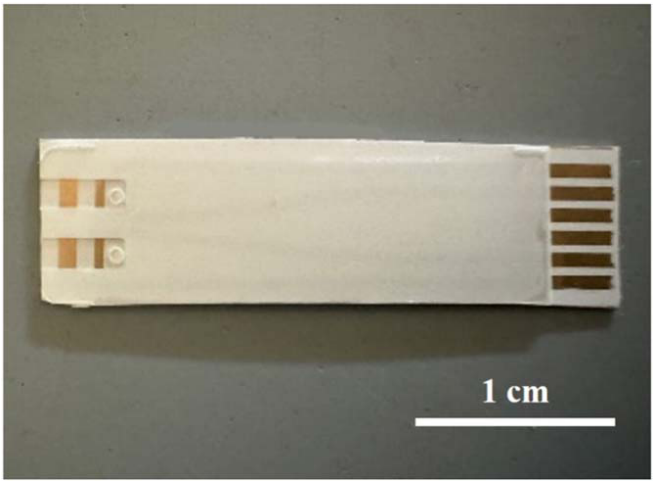

Figure 1. Schematic of the test strip.

In Fig. 3, a printed circuit board (PCB) was meticulously designed to facilitate the conversion of voltage signals obtained from the test strips into digital readings. To amplify the detected signal from the test strip, a metal-oxide-semiconductor field-effect transistor (MOSFET) (STMicroelectronics STP200N3LL) was employed. The PCB comprises components like the pattern generator, reading display, strip connector, and more, and the device operates by connecting a strip to the Arduino-activated system. The Arduino system, an open-source hardware and software platform, facilitates seamless prototyping and development of interactive electronic projects. Comprising a microcontroller board equipped with versatile input/output pins and a user-friendly development environment, Arduino enables coding and uploading directly onto the board.[45,46] The Arduino triggers the pattern generator to create a test pattern, generating output signals through the strip. The readout block, equipped with a MOSFET, amplifies the signal, which is then converted to a frequency signal by a voltage-controlled oscillator (VCO). A counter measures the VCO output, providing a digital representation of the readout voltage displayed on the device. The device employs multiple test patterns for each measurement, averting charge accumulation effects on the strip. Adjustable parameters, including test pattern length and frequency, are controlled by the Arduino and a potentiometer, ensuring adaptability to various strip types. The MOSFET's active socket allows easy replacement for optimization, emphasizing the device's flexibility and precision in concentration measurements.

Results and Discussion

To validate the reliability of the dual-channel sensor and its capability to distinguish between two distinct biomarkers, a series of tests were conducted. Each channel was individually assessed to demonstrate the functionality of both channels. These strips were

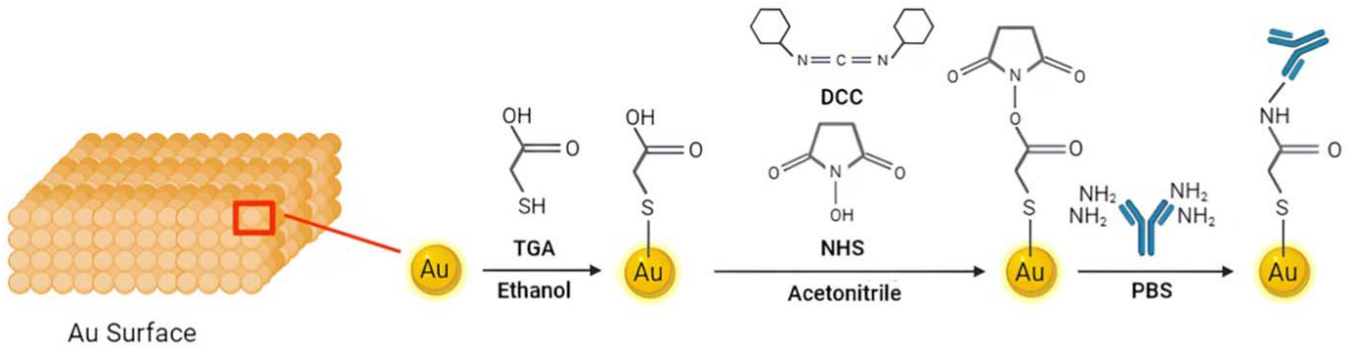

Figure 2. Functionalization step of test strips.

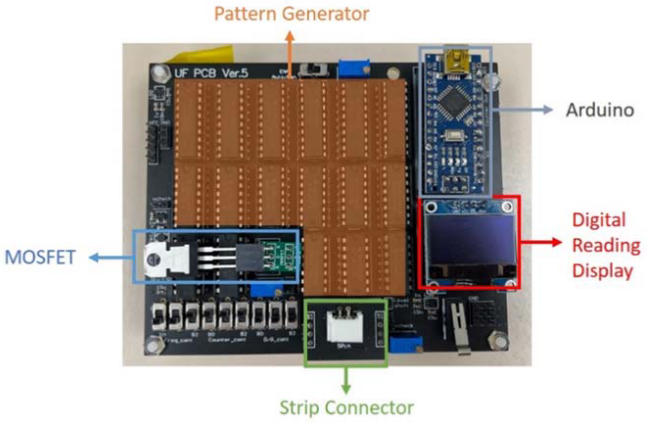

Figure 3. Printed circuit board to generate digital reading.

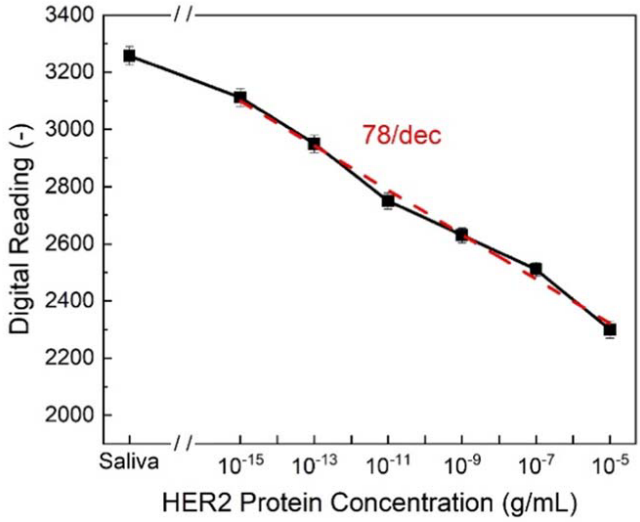

Figure 5. Calibration curve of HER2 protein. The sensitivity is 78/dec while the limit of detection is 10^{-15} g ml^{-1}.

tested with varying concentrations of diluted pure HER2 protein (Sino Biological Inc., Chesterbrook, PA) and CA 15-3 (Sino Biological Inc., Chesterbrook, PA). The dilutions were prepared using pure artificial saliva (Pickering Laboratories Inc., Mountain View, CA), and the proteins were diluted from 1×10^{-15} g ml^{-1} to 1×10^{-5} g ml^{-1}. Once the solution is applied to the channel, the antigen-antibody complexes respond to a pulsed gate electric field by stretching and contracting, resembling double springs. This motion, synchronized with the pulse voltage on the test strip, prompts a change in the protein's conformation. As a result, a time-dependent electric field is applied to the MOSFET gate, leading to a spring-like pattern in the drain voltage waveform, facilitated by the connection between the sensor strip and the MOSFET's gate electrode.[47,48] Figure 4 illustrates the schematic of how the sensor operates. As the protein concentration rises, a concurrent increase in the gate current is observed, resulting in a proportional decrease in the output drain current. Simply put, elevated protein concentration in the sample corresponds to lower output readings. Figure 5 demonstrates that the double channel strip can detect the HER2 in artificial saliva samples, with a limit of detection as low as 1×10^{-15} g ml^{-1}. The HER2 side exhibits a sensitivity of 78/dec. The data presented in this paper are the average of ten measurements, demonstrating reproducibility. Figure 6 shows the result of the human sample test. Sixteen human samples were tested with the strips to validate the technique. The digital reading shows a decline as one moves from the healthy group to the invasive breast cancer group, signifying an elevation in HER2 concentration. In situ breast cancer is an early stage where abnormal cells are confined to the milk ducts or lobules and haven't spread.[49] Invasive breast cancer is a more advanced stage where cancer cells have invaded surrounding breast tissue, posing a greater risk of spreading to other parts of the body. Significantly, the majority of invasive breast cancer samples exhibit HER2-negativity, a determination established through Immunohistochemistry (IHC). The sensor developed in this study boasts a low limit of detection, enabling the differentiation of negative samples. This detection method proved highly effective in distinguishing between diverse sample groups, presenting substantial advantages for early detection and subsequent treatment.

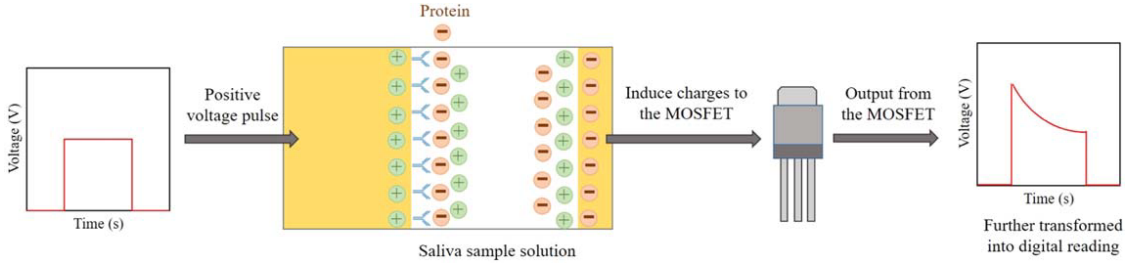

Figure 4. The schematic illustrating the operation of the biosensor.

Table I. Patient characteristics and sensor readings by disease group. Continuous variables presented as median (range); categorical variables presented as N (col%). P-values are the results of Kruskal-Wallis tests (continuous outcomes) and Fisher's exact tests.

	Healthy volunteers (N = 4, 25%)	In situ breast cancer (N = 3, 19%)	Invasive breast cancer (N = 9, 56%)	P value
HER2	3264 (3177, 3355)	3004 (2979, 3147)	2679 (1984, 3380)	0.003
CA 15-3	3196 (3129, 3350)	2874 (2849, 3179)	2770 (1988, 3293)	0.011

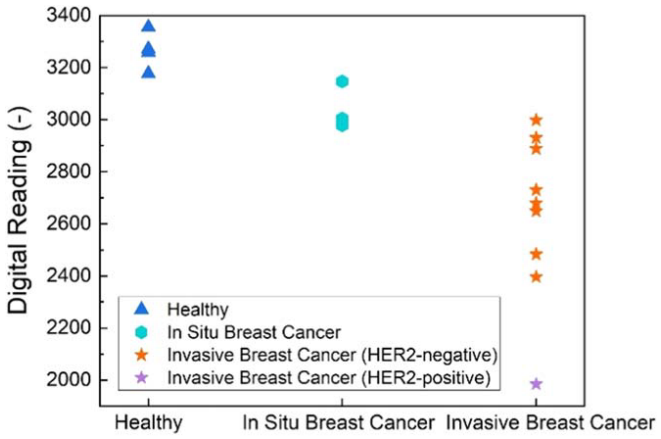

Figure 6. The output digital reading result from the human sample test with strips functionalized by HER2 antibody.

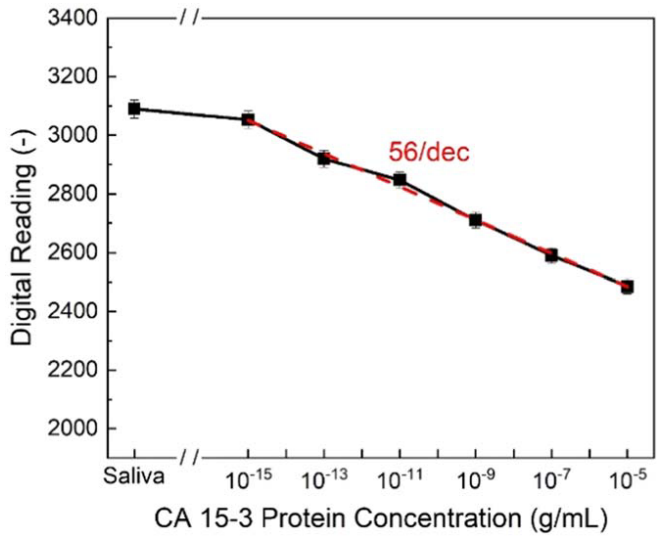

Figure 7. Calibration curve of CA 15-3 protein. The sensitivity is 56/dec while the limit of detection is 10^{-15} g ml^{-1}.

In Fig. 7, the calibration curve for the CA 15-3 side of the dual-channel strip is depicted. The sensitivity is approximately 56/dec, while the limit of detection reaches as low as 10^{-15} g ml^{-1}. To underscore the relevance of the sensor, human sample testing was conducted, and the results are illustrated in Fig. 8. The calibration curve, coupled with the human sample test readings, provides individuals with valuable insights into their health status. A decrease in readings may warrant caution, signaling an increase in breast cancer-related biomarkers. Simultaneous testing of both biomarkers enhances the accuracy of the rapid breast cancer test, offering a comprehensive understanding of one's health.

Table I shows the analytical result of HER2 and CA 15-3 human sample test. The p-values for HER2 and CA 15-3 were 0.003 and 0.011, respectively. In simpler terms, these values indicate the likelihood that the observed differences in the levels of HER2 and CA 15-3 between healthy individuals and cancer patients are not due

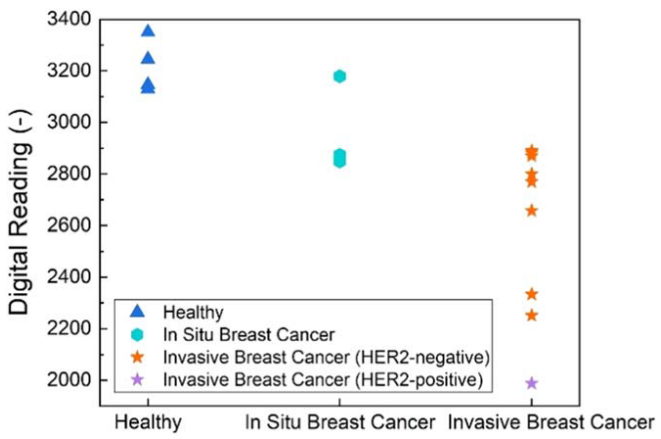

Figure 8. The output digital reading result from the human sample test with strips functionalized by CA 15-3 antibody.

to random chance. Lower p-values, such as 0.003, suggest a higher level of statistical significance, implying that the observed differences are more likely to be real and not just random variations. While caution is warranted due to the study's small sample size and demographic imbalances, these p-values provide a foundation for further investigation into the relevance of HER2 and CA 15-3 as potential biomarkers for distinguishing between health and cancer within the studied population.

Conclusions

The introduction of the dual-channel strip represents a significant advancement in breast cancer detection methodology. The innovative design, capable of simultaneously assessing HER2 and CA 15-3 biomarkers, enhances the precision of rapid breast cancer testing. The functionalization process, involving specific antibodies and thorough validation, ensures reliability and specificity in detecting targeted proteins. The sensitivity and low limit of detection demonstrated by the dual-channel strip, coupled with successful human sample testing, underscore its potential as a valuable diagnostic tool. The ability to differentiate between healthy and breast cancer samples offers a comprehensive understanding of one's health status, potentially revolutionizing early detection strategies. Completing the entire test in under two seconds, this technique is poised to greatly assist medical professionals in conducting breast cancer screening tests, whether in a hospital setting or public areas. The sensor's disposable design promotes sustainability by reducing environmental impact, conserving resources in manufacturing, simplifying waste management, and ensuring hygiene standards in healthcare. Furthermore, as this technology gains traction, it opens doors for broader applications in cancer diagnostics and beyond. Its adaptability and efficiency could pave the way for similar advancements in detecting other types of cancer and even non-cancerous conditions, thereby transforming the landscape of medical diagnosis.

Acknowledgments

This research was partially funded by NIH-NIDCR Grant R56 DE025001.The authors at National Yang Ming Chiao Tung University, Hsinchu 30010, Taiwan would like to thank the

National Science and Technology Council, Taiwan, for their financial support under the grants NSTC 112–2628-E-A49–015.

Ethics Approval

Human samples were obtained through the University of Florida Clinical and Translational Science Institute (UF CTSI) Biorepository. These de-identified samples all came with corresponding diagnoses, which were confirmed through biopsies as part of the patients' routine care (UF IRB202101643).

ORCID

Hsiao-Hsuan Wan https://orcid.org/0000-0002-6986-8217
Chao-Ching Chiang https://orcid.org/0000-0002-0447-8170
Xinyi Xia https://orcid.org/0000-0002-8644-8599
Jian-Sian Li https://orcid.org/0000-0002-2817-7612

References

1. R. Gidwani, J. A. Franks, E. M. Enogela, N. E. Caston, C. P. Williams, M. S. Aswani, A. Azuero, and G. B. Rocque, *JCO Oncology Practice*, **18**, e235 (2022).
2. C.-f D. C. Prevention, (2023), https://cdc.gov/breast-cancer/about/?CDC_AAref_Val=https://www.cdc.gov/cancer/breast/basic_info/index.htm.
3. R. L. Siegel, K. D. Miller, N. S. Wagle, and A. Jemal, *Ca Cancer J Clin*, **73**, 17 (2023).
4. A. C. Society, (2024), https://cancer.org/cancer/types/breast-cancer/about/how-common-is-breast-cancer.html.
5. E. Klinger, *Cancer Costs and Options for Care in the United States* (2021), https://biosimilarscouncil.org/resource/cancer-costs-in-the-united-states/.
6. S. Kaur, M. J. Baine, M. Jain, A. R. Sasson, and S. K. Batra, *Biomarkers in medicine*, **6**, 597 (2012).
7. N. P. Gupta, P. K. Malik, and B. S. Ram, *International conference on computation, automation and knowledge management (ICCAKM)," p. 42–46. IEEE, 2020* (2020).
8. K. R. Khondakar, M. A. Kachouei, F. E. Erukainure, and M. A. Ali, *ECS Sensors Plus*, **2**, 043403 (2023).
9. N. Aristokli, I. Polycarpou, S. Themistocleous, D. Sophocleous, and I. Mamais, *Radiography*, **28**, 848 (2022).
10. S. Azhdeh, A. Kaviani, N. Sadighi, and M. Rahmani, *European Journal of Breast Health*, **17**, 53 (2021).
11. H. Liu, H. Zhan, D. Sun, and Y. Zhang, *BMC Med. Imaging*, **20**, 1 (2020).
12. R.-d O. Pereira, L. A.-D. Luz, D. C. Chagas, J. R. Amorim, E.-d J. Nery-Júnior, A. C.-B. R. Alves, F. T.-D. Abreu-Neto, M.-d C. B. Oliveira, D. R.-C. Silva, and J. M. Soares-Júnior, *Clinics*, **75**, 1805 (2020).
13. S. E.-M. Tolibia, A. Galdámez-Martínez, R. A. Salinas, and A. Dutt, *ECS Sensors Plus*, **2**, 044601 (2023).
14. D. X. Assad, E. C.-P. Mascarenhas, A. G.-C. Normando, H. Chardin, G. B. Barra, R. Pratesi, Y. K.-D. M. Nobrega, A. C. Acevedo, and E. N.-S. Guerra, *Molecular and clinical oncology*, **13**, 155 (2020).
15. S. Jeong, M.-J. Park, W. Song, and H.-S. Kim, *Clin. Biochem.*, **78**, 43 (2020).
16. P. Ranjan, A. Parihar, S. Jain, N. Kumar, C. Dhand, S. Murali, D. Mishra, S. K. Sanghi, J. Chaurasia, and A. K. Srivastava, *Anal. Biochem.*, **610**, 113996 (2020).
17. M. Koopaie, M. Fatahzadeh, S. Kolahdooz, and R. Mousavi, *Current Women's Health Reviews,*, **19**, 48 (2023).
18. I. A. Nemeir, *Development of new bioanalytical tool for the detection and monitoring of breast cancer biomarkers via saliva* (HAL Open Science, Lyon , France) (2020).
19. H. E. Tarek, M. M. Ellithy, R. A. Morsy, D. El-Lebedy, R. M. Abbas, and H. N. Shalash, *Journal of The Arab Society for Medical Research*, **17**, 132 (2022).
20. E. C. Porto-Mascarenhas, D. X. Assad, H. Chardin, D. Gozal, G. D.-L. Canto, A. C. Acevedo, and E. N.-S. Guerra, *Critical reviews in oncology/hematology*, **110**, 62 (2017).
21. F. Laidi, A. Bouziane, A. Errachid, and F. Zaoui, *Asian Pacific Journal of Cancer Prevention*, **17**, 335 (2016).
22. F. Laidi and F. Zaoui, *Journal of International Dental and Medical research*, **8**, 94 (2015).
23. Y. Yarden, *Oncology*, **61**, 1 (2001).
24. S. Tang, L. Wei, Y. Sun, F. Zhou, S. Zhu, R. Yang, Y. Huang, H. Zhang, H. Xu, and J. Yang, *PLoS One*, **11**, e0163030 (2016).
25. L. Jardines, *The American surgeon*, **62**, 119 (1996).
26. H.-H. Wan, H. Zhu, C.-C. Chiang, J.-S. Li, F. Ren, C.-T. Tsai, Y.-T. Liao, D. Neal, J. F. Esquivel-Upshaw, and S. J. Pearton, *J. Vac. Sci. Technol. B*, **42**, 023202 (2024).
27. P. H. Carey, B. C. Lobo, M. P. Gebhard, M. E. Leon, S. D. Flax, N. S. Harris, Y.-T. Liao, C.-W. Chang, J. Lin, and F. Ren, *J. Electrochem. Soc.*, **167**, 037507 (2019).
28. P. H. Carey, J. Yang, F. Ren, Y.-T. Liao, C.-W. Chang, J. Lin, S. J. Pearton, B. Lobo, and M. E. Leon, *J. Electrochem. Soc.*, **166**, B708 (2019).
29. K. Chen, B. Kang, H. Wang, T. Lele, F. Ren, Y. Wang, C. Chang, S. Pearton, D. Dennis, and J. Johnson, *Appl. Phys. Lett.*, **92**, 192103 (2008).
30. J. Yang, P. Carey IV, F. Ren, M. A. Mastro, K. Beers, S. Pearton, and I. I. Kravchenko, *Appl. Phys. Lett.*, **113**, 032101 (2018).
31. M. Xian, P. H. Carey, C. Fares, F. Ren, S.-S. Shan, Y.-T. Liao, J. F. Esquivel-Upshaw, and S. J. Pearton, *in 2020 IEEE Research and Applications of Photonics in Defense Conference (RAPID),* (IEEE) p. 1–2 (2020).
32. M. Xian, H. Luo, X. Xia, C. Fares, P. H. Carey, C.-W. Chiu, F. Ren, S.-S. Shan, Y.-T. Liao, and S.-M. Hsu, *J. Vac. Sci. Technol. B*, **39**, 033202 (2021).
33. ACROBiosysteams. Human Mucin-1, Fc Tag ELISA (https://acrobiosystems.com/L-380-Mucin-1.html?gclid=EAIaIQobChMIz5Wuwe6EgQMVdUd_AB1BbQZXEAAYASAAEgKlUPD_BwE.
34. V. Agnolon, A. Contato, A. Meneghello, E. Tagliabue, G. Toffoli, M. Gion, F. Polo, and A. S. Fabricio, *Sci. Rep.*, **10**, 3016 (2020).
35. N. K. Stout, S. J. Lee, C. B. Schechter, K. Kerlikowske, O. Alagoz, D. Berry, D. S. Buist, M. Cevik, G. Chisholm, and H. J. De Koning, *Journal of the National Cancer Institute*, **106**, dju092 (2014).
36. National Research Council, Institute of Medicine, Policy and Global Affairs, Board on Science, Technology and Economy Policy, National Cancer Policy Board, and Committee on New Approaches to Early Detection and Diagnosis of Breast Cancer, *Saving Women's Lives: Strategies for Improving Breast Cancer Detection and Diagnosis*, ed. D. B. Petitti, E. E. Penhoet, and J. E. Joy (National Academy of Science, Washington, DC) (2005).
37. R.-I. Stefan-van Staden, *ECS Sensors Plus*, **1**, 011603 (2022).
38. M. Xian, J. L. Stephany, C.-W. Chiu, C.-C. Chiang, F. Ren, C.-T. Tsai, S.-S. Shan, Y.-T. Liao, J. F. Esquivel-Upshaw, and S. J. Pearton, *J. Vac. Sci. Technol. B*, **41**, 013201 (2023).
39. C.-C. Chiang, C.-W. Chiu, F. Ren, C.-T. Tsai, Y.-T. Liao, J. F. Esquivel-Upshaw, and S. J. Pearton, *J. Vac. Sci. Technol. B*, **41**, 012204 (2023).
40. C.-C. Chiang, C.-W. Chiu, F. Ren, C.-T. Tsai, Y.-T. Liao, J. F. Esquivel-Upshaw, and S. J. Pearton, *ECS J. Solid State Sci. Technol.*, **11**, 105007 (2022).
41. H. Shrivastava and G. V. Tcheslavski, *International Journal of Biometrics*, **10**, 52 (2018).
42. G. J. Besseris, *International Journal of Quality & Reliability Management*, **26**, 341 (2009).
43. R. M. Flikkema, A. H. Toledo, R. Anaya-Prado, and L. H. Toledo-Pereyra, *Journal of Investigative Surgery*, **24**, 237 (2011).
44. M. Qualls, D. J. Pallin, and J. D. Schuur, *Academic Emergency Medicine*, **17**, 1113 (2010).
45. J. J. López and P. Lamo, *Sensors*, **23**, 7511 (2023).
46. J. Bhandarkar, G. Halde, and S. Parihar, *Open Access Repository*, **10**, 87 (2023).
47. J. Yang, P. Carey, F. Ren, M. A. Mastro, K. Beers, S. Pearton, and I. I. Kravchenko, *Appl. Phys. Lett.*, **113** (2018).
48. H.-H. Wan, H. Zhu, C.-C. Chiang, J.-S. Li, F. Ren, C.-T. Tsai, Y.-T. Liao, D. Neal, J. F. Esquivel-Upshaw, and S. J. Pearton, *J. Vac. Sci. Technol. B*, **42** (2024).
49. S. Sornambikai, H. Amir, G. Bhuvaneshwari, N. Ponpandian, and C. Viswanathan, *ECS Sensors Plus*, **1**, 021602 (2022).